Excitation density in time-resolved water window soft X-ray spectroscopies: Experimental constraints in the detection of excited states

R. Costantini [a], A. Morgante [a,b], M. Dell'Angela [a,*]

[a] *CNR-IOM, Strada Statale 14 – km 163.5, 34149 Trieste, Italy*
[b] *Physics Department, University of Trieste, Via Valerio 2, 34127 Trieste, Italy*

A B S T R A C T

Time-resolved X-ray spectroscopies have the potential of unveiling ultrafast processes with chemical sensitivity, but their widespread application is still withheld by technical and experimental constraints on two levels: the count rate and the amount of signal to be measured. In this paper, we will give a brief overview of the available pulsed X-ray sources focusing in particular on those delivering photons with energies inside the water window (280–550 eV), thus allowing to access the C1s, N1s and O1s core levels which are relevant for the characterization of thin organic films and small molecules adsorbed on surfaces. We will mainly discuss the photon fluxes delivered by such sources in relation to their repetition rates, and we will see how these factors affect time-resolved measurements. The main purpose of this work is to discuss the most crucial parameter to adjust in pump-probe spectroscopies: the excitation density, which corresponds to the fraction of photoexcited molecules/atoms. We show that such quantity may be increased up to roughly 25% in gas phase and other robust samples, however, due to a lower damage threshold, in organic films it is typically constrained to be in the order of 1–5%. Despite the initially limited population of excited states in the latter case, we show that the evolution of the system may lead to a collective response of the material, which entirely modifies the measured core level line shape, thus providing a clear signal that may nonetheless offer valuable insights into the dynamics of the studied process.

1. Introduction

In the fields of optoelectronics and photochemistry there is growing interest in studying the response to optical excitations of organic molecules, films and interfaces, as these systems are of fundamental relevance for the development of the next generation of environmentally sustainable optoelectronic devices and catalysts. The invention of the laser in 1960 and the steady developments in its technology through the years are closely correlated to the advances in time-resolved spectroscopies. The advent of Ti:sapphire lasers in the early nineties and their commercial availability, for instance, resulted in huge progress in the characterization of ultrafast (<100 fs) physical processes [1–3]. Similarly, the strive for the generation of soft X-ray pulses in the water window (280–550 eV) allowed to extend the pump-probe approach to X-ray absorption [4–9] and photoemission [10–16] spectroscopies at the C, N and O 1 s core levels, paving the way for studying sub-nanosecond dynamics in organic films and interfaces with chemical sensitivity. Nowadays, the different sources delivering soft X-ray pulses are

high-harmonic generation and laser plasma setups, free electron lasers and synchrotrons [17]. In the following section, we will briefly review and analyze the typical working parameters of the above-mentioned sources when it comes to time-resolved spectroscopies using water window soft X-rays.

We will then discuss and calculate the excitation density for pump-probe measurements. Such quantity can be written in terms of the percentage of photoexcited molecules (or atoms) in the probed volume and is directly proportional to the applied pump fluence (i.e., the optical energy per unit area). Theoretically, high excitation densities translate to a good signal-to-noise ratio (SNR), but the appearance of nonlinear effects and sample damage above certain fluence thresholds may negatively affect the measurements. We will show that these factors impose upper limits to the excitation density, which in gas phase measurements may reach up to 25%, while they translate to a maximal fraction of excited molecules in the order of 1–5% in organic heterojunctions, which makes the detection of excited states via time-resolved X-ray spectroscopies more challenging. As we will see, the number of counts

---

* Corresponding author.
  E-mail address: dellangela@iom.cnr.it (M. Dell'Angela).

required to discriminate the small fraction of excited states in the sample varies with the inverse square of the excitation density; therefore, it emerges that one of the most important developments in pulsed soft X-ray sources is the increase of the repetition rates, which will allow faster measurement and a less tedious data analysis because of the averaging of single shot fluctuations.

2. Sources of pulsed soft X-ray radiation

The discovery of X-rays has had a huge impact on our fundamental understanding of matter. It was soon noted that their short wavelength could be exploited for imaging the interior of a specimen, for examining the atomic structure through diffraction techniques and for characterizing the local chemical and structural environment of selected elements via a number of X-ray spectroscopies. Over the past few decades, the development of pulsed X-ray sources has opened the way for the exploration of the time domain using these techniques, allowing scientists to investigate in real time the physical and chemical processes with the elemental sensitivity offered by soft X-rays. Before proceeding with the overview on the pulsed X-ray sources, it is important to define the boundaries of the soft X-ray region to avoid any ambiguity. The term soft X-ray is commonly used to refer to the photon energy range between few hundreds of eVs to few keVs, but the line separating the soft X-rays from the extreme ultraviolet (EUV/XUV) is often blurry: it is usually placed at about 100 eV, in the book by D. Atwood it is placed at 250 eV [18], but several works in which few tens of eVs are identified as soft X-rays can also be found. In this paper, we will consider only a smaller portion of the soft X-ray region: the water window. This term refers to the portion of the electromagnetic spectrum in which water is transparent to X-rays, which extends approximately from 280 to 550 eV, comprising the C, N and O 1 s core levels, and it is therefore the photon energy range relevant for the study of organic molecules and interfaces for photochemistry and optoelectronics. For this reason, in the following overview we will solely discuss the sources providing X-ray pulses in the water window, and we refer the reader elsewhere for a more complete discussion on the topic [17].

Pulsed X-ray radiation can be produced at high-harmonic generation (HHG), plasma and accelerator based sources as free electron lasers (FELs) and synchrotrons. In HHG a laser beam is focused into a gas jet, leading to the generation of ultrashort pulses with photon energies that have been gradually increased to cover the water window [19–21]. In plasma X-ray sources, femtosecond X-ray pulses are obtained by focusing a high-power laser on a solid target [22]. Although some proof-of-concept studies of pulsed soft X-rays obtained with these sources have already been performed [23–35], they are still in and early development stage and will not be further discussed here. FEL radiation is produced by injecting a high-energy electron bunch into a series of undulators; the interaction of the electron bunch with the emitted radiation field results in the appearance of a micro-bunch structure, and to a following emission of a coherent and intense beam of X-ray photons [36,37]. At synchrotrons, multiple electron bunches are accumulated in the storage ring and radiation is generated at every revolution inside the insertion devices, which can be bending magnets, wigglers or undulators. Special filling patterns of the storage ring have been implemented to produce a single X-ray pulse separated from the conventional multibunch radiation, allowing to perform time-resolved X-ray spectroscopies at MHz repetition rates [11,38–40].

2.1. High-harmonic generation

The recent advances in laser technology made the table-top generation of X-ray pulses possible via high-harmonic generation. In HHG a femtosecond laser beam is focused into a high-pressure waveguide (or a jet [41,42]) filled with a noble gas; when the intensity of the driving laser is high enough, the emission from many atoms adds constructively and the IR photons are upconverted to EUV or soft X-ray sub-femtosecond pulses, which for increasing photon energy (i.e., increasing harmonic number) merge into a broadband supercontinuum spectrum. In such process, phase matching is required to coherently amplify the signal of the many body emission in the medium. It can be demonstrated that such favorable condition is only obtainable below a critical ionization level in the gas, indicating the presence of a phase matching cutoff $\propto \lambda_L^{1.7}$ [43,44], where λ_L is the wavelength of the driving laser. The same $\lambda_L^{1.7}$ scaling persists when evaluating the highest energy harmonic achievable in the HHG process, which gives a limit of ~150 eV when using $\lambda_L = 0.8$ μm from Ti:sapphire lasers as drivers. Higher photon energies can be achieved by driving the HHG with mid-IR pulses: with a driving wavelength of $\lambda_L = 3.9$ μm the successful generation of soft X-rays up to 1600 eV has been demonstrated [45]. By using analogous approaches several setups covering the carbon (270–320 eV) and nitrogen (390–430 eV) K-edge absorption edges have been presented [44,46–56].

As a rule of thumb, harmonic generation in the water window requires driving pulse energies of few mJ or few-cycle laser pulses, thus dictating stringent conditions on the operating parameters of HHG systems. In the first case if we consider a commonly available femtosecond laser of about 20 W average power, it corresponds to 20 mJ at 1 kHz at the source and 2 mJ in the gas cell; in order to have the same pulse energy at 1 MHz an impractical average power of 20 kW is needed. Soft X-ray HHG systems inherit the repetition rate from the driving lasers, and can thus be commonly developed to operate at 1 kHz [46,47,51,55,57] or lower [48,57]. The supercontinuum emission spectra and the high number of photons per pulse ($>10^6$ in setups covering the carbon K-edge) are a valuable advantage in transient soft X-ray absorption experiments, especially when measured in transmission through gas phase [9,46,58], liquid [47] or thin film [56,59] samples. Remarkably, repetition rates of 100 kHz have been reported very recently by M. Gebhardt et al. following a novel approach based on a thulium-doped fiber laser [60].

2.2. Free electron lasers

In FELs, a bunch of relativistic electrons pass through a periodic array of magnets, the undulator, generating an electromagnetic wave, and the interaction of the electrons with the latter results in the amplification of the radiation generated inside the undulator [37]. This process is called self-amplified spontaneous emission (SASE) and is the principle on which most FELs are based [61–64]. However, as it originates from the incoherent and spontaneous radiation of the relativistic electron bunch, SASE is characterized by high shot-to-shot fluctuations, both in intensity and in spectral shape. To overcome this issue, one solution is to use the high harmonics of external seed laser to modulate the electron beam for creating a microbunched structure before the injection into the final undulator. This is the high-gain harmonic generation (HGHG) approach, on which the FERMI FEL (Italy) is based [65]. The intensity of FEL radiation increases exponentially along the undulator, to eventually deliver short (10–100 fs) EUV or soft X-ray pulses with unmatched peak brilliance, in the order of 10^{11}-10^{12} photons per pulse, which proved to be a huge benefit for diffraction techniques such as femtosecond protein crystallography [66,67]. The drawback of FELs high peak brilliance is that a single pulse may induce a Coulomb explosion that instantly destroys the specimen, thus forcing the users either to measure in gas phase and liquid jets or to raster scan the surface of a finite sample during the acquisition. Moreover, a high number of ionizing photons is undesirable for photon-in/electron-out spectroscopies, such as X-ray photoemission, since it is likely to introduce space charge artifacts [64,68–70]. Therefore, with few limited exceptions, the FEL intensity is often reduced during the measurements to minimize sample damage and other unwanted effects.

FELs currently operate at repetition rates ranging from few Hz to 120 Hz. Few of them present a more complex temporal pattern obtained by modulating electron bunches in order to repeatedly produce a train with

a certain number of FEL pulses at a few Hz rate. As a consequence, the measurements times can be shorter and it is not necessary to perform elaborate shot-to-shot acquisition modes to normalize the beam fluctuations. At the FLASH FEL (Germany), for instance, it is possible to generate hundreds of pulses at a few Hz [64], resulting in a cumulative pulse rate approaching 8 kHz. With an analogous approach, the recently commissioned European XFEL (Germany) should be able to generate up to 2700 pulses at a repetition rate of 10 Hz [71], therefore pushing the cumulative rate up to ~30 kHz. Groundbreaking advances will be soon brought by the upgrade of LCLS (USA) to LCLS-II, which promises to deliver a continuous bunch repetition rate of 1 MHz [72].

2.3. Synchrotrons

Synchrotron radiation is generated when relativistic electrons are accelerated through strong magnetic fields, that can be applied using insertion devices as bending magnets, wigglers or undulators. As opposed to FELs, in which the electron bunches are dumped after the undulator, at synchrotrons the electrons are accumulated in the storage ring, where their kinetic energy is kept constant, and pass through the insertion devices more than a million times per second, allowing multiple users to work simultaneously. These facilities offer collimated, tunable X-ray beams with high spectral brilliance, in the order of 10^{13} photons/s, therefore implying a massive reduction of acquisition times and a significant increase in signal-to-noise ratio if compared to other sources. Even though the average photon flux of synchrotrons is similar to that of the other pulsed X-ray sources, the electron filling pattern in the storage ring, which determines the temporal structure of the photon pulses, typically consists in hundreds of bunches separated by few nanoseconds (~500 MHz), thus bringing the peak flux to roughly 10^4 photons per pulse, which is low enough to avoid unwanted non-linear effects.

For instrumental requirements, the so-called multibunch electrons are always followed by an unfilled dark gap of at least 100 ns, in which an isolated bunch (camshaft) can be placed. With such hybrid filling pattern, it is possible to use gated detectors to discriminate the signal coming from the camshaft and to design time-resolved experiments. For this purpose, pulsed lasers synchronized to the storage ring are typically used to photoexcite the sample, and the relaxation dynamics of the studied systems are monitored as a function of the delay time between the optical pump and the isolated X-ray probe pulses [11,38–40]. With this approach it is possible to perform time-resolved measurements at repetition rates in the order of 1 MHz (the revolution frequency of storage rings) with the advantage of having highly stable and easily tunable X-ray pulses as a probe. A critical constraint, however, is represented by the temporal resolution that is normally achievable at synchrotrons, which is limited by the electron bunch length to 50–100 ps, thus making it impossible to access chemical reactions, phase transitions, charge transfer processes and other phenomena that occur on sub-ps time scales.

A few solutions have been proposed to modify the temporal structure of the electron bunches in storage rings in order to obtain shorter pulses, in particular by changing the momentum compaction factor (via low-α operation modes) [73], by laser-induced modulation of the electron bunches ("femtoslicing") [74], or by deflecting the electron orbit with crab cavities [75,76]. The low-α mode can in principle be implemented at any synchrotron by properly tuning the existing electron optics, allowing to generate X-ray pulses as short as a few ps. Its operation, however, requires very low ring currents (roughly 20 times lower than in standard conditions), in contrast with the need for high photon fluxes of the majority of synchrotron users; at BESSY II (HZB, Germany), for this consideration, only 2 weeks of low-α operation are offered each year. Femtoslicing has been successfully demonstrated with the generation of ~100 fs pulses at Advanced Light Source (ALS, Berkeley, USA) [77], BESSY II [78], Swiss Light Source (PSI, Switzerland) [79] and SOLEIL (France) [80], but with low (few kHz) repetition rate of these

setups, inherited from the modulating lasers. The implementation of crab cavities has been planned for the Advanced Photon Source (APS, Argonne, USA) upgrade, where it is supposed to bring the pulse duration to less than 2 ps [76], and is also being discussed for the ELETTRA (Italy) synchrotron upgrade. Finally, an innovative scheme has been proposed at BESSY II, which is known as the VSR project [81]. It is based on the introduction of additional superconducting RF cavities, operating at higher harmonics of the nominal 500 MHz, which would introduce beating frequencies that result in a modulation of the temporal structure of the electron bunches. In particular, this will lead to the emission of alternate short (few ps) and long X-ray pulses without affecting the average brightness, and in combination with the low-α operation is expected to deliver pulses of sub-ps length.

Despite the expected advances in the generation of short pulses at synchrotrons, sub-ps dynamics will still be accessible only at FELs and HHG setups in the near future. Thanks to the ease of access to synchrotrons and their higher repetition rates, however, these sources represent a valid alternative for the characterization of physical processes in the pico- to nanosecond timescales.

3. Experimental constraints in pump-probe water window soft X-ray spectroscopies

The signal-to-noise ratio in pump-probe measurements is determined by both pump and probe parameters. Regarding the pump, the most important figure to consider is the applied fluence, i.e., the pulse energy per unit area, which determines the excitation density in the sample and thus the amount of signal that can be measured; this aspect will be addressed later in the section. The probe, on the other hand, determines the integration time required to obtain a clear identification of the measured excited state.

3.1. Probe: the count rate

On a first approximation, higher photon fluxes translate into faster acquisitions, with the caveat that the number of photons per pulse must be below a certain threshold. In our analysis we consider nonlinear processes as unwanted effects and therefore we will not address nonlinear spectroscopies. Given the combination of different X-ray spectroscopies, available water window soft X-ray sources described in previous paragraph and detection methods, it is not possible to derive a general rule and a few examples may be of use. First of all, we can divide the techniques into two categories: photon-in/photon-out and photon-in/electron-out. In the latter, since charged particles are detected, the measurement will be affected by the presence of electromagnetic fields between the sample and the analyzer, therefore imposing more stringent constraints on the number of photons per pulse in order to avoid space charge effects [64,68–70]. As an example, with 10^4 photons per pulse, a typical flux at synchrotrons, the Fermi edge of a metal shifts in the order of 10 meV [69], which is a tolerable artifact for most photoemission studies. We have shown in the previous section that both HHGs and FELs have higher peak brilliances, therefore the incoming probe beams of these sources must be filtered for performing photoemission spectroscopies. When employing modern electron spectrometers equipped with delay line detectors only one electron per pulse can be counted and therefore the possibility of increasing the repetition rate becomes crucial to increase the count rate [82,83]. On the other hand, when employing traditional hemispherical analyzers equipped with CCD (charge-coupled device) detectors 10–100 times more signal can be integrated, depending on the number of pixels. In such case, if the space charge effects do not affect the spectra, measuring at high repetition rate with low flux is equivalent to measure at low repetition rate with high flux. Besides the appearance of space charge effects, it is important to underline that the X-ray probe photons can also cause radiation damage to organic samples, which may occur with beam intensities even lower than those causing space charge, therefore it is crucial to optimize the detection of
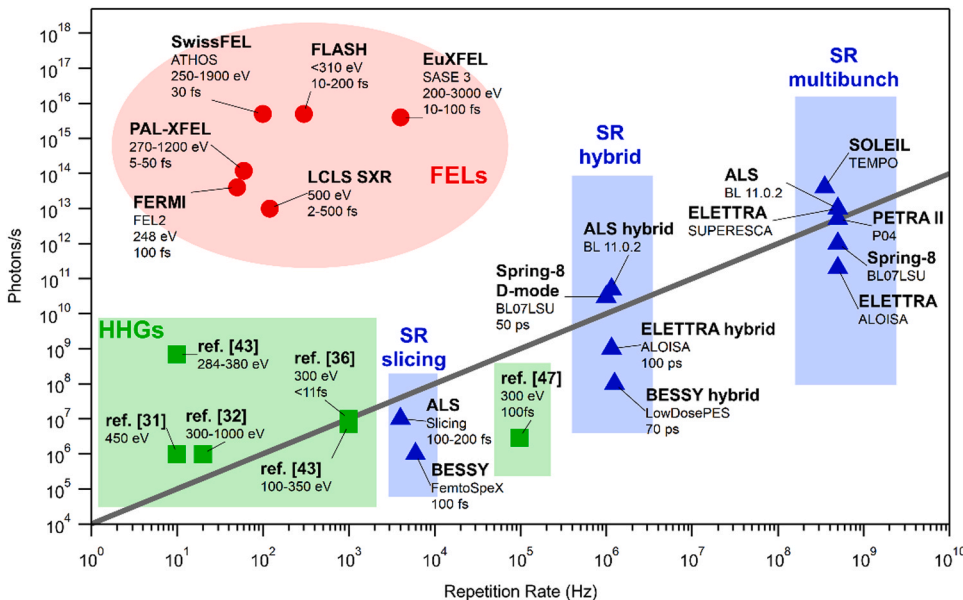
Fig. 1. Photon flux for a set of X-ray facilities. The average photon fluxes of few selected HHGs (green squares), FELs (red circles) and synchrotrons (blue triangles) are plotted as a function of the source repetition rate. The gray solid line represents the space charge onset for photoemission measurements of 10^4 photons per pulse. FELs and HHGs are consistently found above such line, while synchrotrons are typically below, especially at beamlines devoted to time-resolved measurements. Note that synchrotron fluxes are given per unit of the 0.1% of the bandwidth and FEL fluxes are given considering the full bandwidth (few percent in SASE) as they are usually monochromatized for performing soft X-ray spectroscopies. HHGs in the water window operate with non-monochromatized broadband pulses, therefore the parameter given here is the total photon flux. Photon flux for a set of X-ray facilities.

the signal. The choice of spectrometer and detector for time-resolved measurements should therefore ensure the best measured counts to incoming probe flux ratio, in order to minimize sample damage.

Photon-in/photon-out techniques, on the other hand, benefit from high peak brilliances. With a HHG source, for instance, it is possible to acquire an X-ray absorption spectrum by detecting the transmitted intensity of just 10^2-10^3 broadband pulses through a thin film sample. The threshold on the photons per pulse in photon-in/photon-out techniques is limited by sample damage, assuming that such threshold is lower than the photon density that introduces nonlinear effects, and therefore depends on the studied system: for some molecular films the low damage threshold may require a pulse energy even lower than the one typically found at synchrotrons, while higher pulse energies can be used for bulk metals or semiconductors. Even in the latter cases, however, FEL pulses at full power are known to permanently transform the structure of the material [84] and the beam intensity has to be significantly reduced to acquire a spectrum.

In Fig. 1 we show the operating parameters of a number of state-of-the-art water window soft X-ray sources, to give a visual summary of the photon fluxes and repetition rates at these facilities. Here, we have drawn a gray solid line that corresponds to the space charge onset of 10^4 photons per pulse, corresponding to a spectral shift of 10 meV mentioned above [69]. Space charge effects depend not only on the number of photons per pulse but also on the dimension of the X-ray spot and on the X-ray pulse lenght [68]. For the sake of simplicity in drawing the space charge onset in Fig. 1 we make the reasonable assumption of all the sources having similar spot sizes and we do not consider X-ray pulse lengths. However, X-ray durations longer than 100 ps obtained at some synchrotrons can cause spectral deformations even for a number of photons per pulse below the space charge onset. Such effects have recently been studied in ref. [85] but can be discarded for this general discussion. In a typical experiment the accepted photon flux needs to be appropriately chosen by considering that on one side photon fluxes above the space charge onset introduce effects in the line shape of photoemission spectra, while on the other side low photon fluxes at low repetition rates correspond to high integration times. HHGs (green squares) with photon energies in the water window are found in the bottom left corner of the graph, with the only exception of the novel setup by Gebhardt et al. [60] based on a thulium-doped fiber laser. Most of the setups reported in the literature have limited repetition rates and their broadband emission spectrum can be efficiently exploited for transient X-ray absorption measurements. FELs (red circles) intrinsically

have outstanding peak brilliances which exceed not only the space charge onset, but also cause the Coulomb explosion of the samples. The beam intensity has to be usually reduced by several orders of magnitude to prevent instantaneous sample degradation, and in photoemission experiments such procedure always involves the space charge minimization. Most synchrotrons (blue triangles) in their multibunch modes operate at about 500 MHz, and they offer average photon fluxes comparable to those of FELs while lying closer to the space charge onset. For time-resolved measurements synchrotrons are either run in the hybrid mode, in which the repetition rate corresponds to the revolution frequency of the storage ring and is ~1 MHz, or a few selected bunches are sliced by a femtosecond laser; the latter method produces shorter pulses, but it is more complex to set up and operate and runs at a repetition rate that is lower by more than 2 orders of magnitude.

Both when detecting electrons and photons, the challenge in pump-probe spectroscopies resides on the fact that the pump-induced signal is usually coming from a small fraction of excited molecules/atoms and it is much weaker than the signal emitted by the unpumped centers in the probed volume, which represents an unwanted background for time-resolved measurements. In the next paragraph we will see that in organic thin films the excited molecules are typically only 1–5%. The acquisition for each delay point should run until the time-dependent signal is sufficiently higher than the statistical noise in the spectrum. To provide a rough estimate we assume that the optical excitation introduces a new component near to a known resonance in the measured spectrum hence we take C as the number of counts in the spectrum, $\sqrt{C}$ as the statistical error associated to it and ρ_{ex} as the excitation density, which we define as the fraction of excited centers at time zero in the probed volume. At zero delay, provided that the probed volume is smaller than the pumped volume and that the excited state lifetime is longer than the probe pulse width, the number of pump-induced counts will be $C\rho_{ex}$; to easily discriminate such counts after the static background subtraction, the latter value should be greater than $3\sqrt{C}$. The inequality therefore becomes:

$$C \gtrsim \frac{9}{\rho_{ex}^2} \tag{1}$$

The quadratic dependence on the excitation density underlines how crucial such parameter is for pump-probe measurements: as we will show in the next section, common values for ρ_{ex} are in the 1–10% range, meaning that to acquire a single spectrum a minimum of roughly 10^3 to
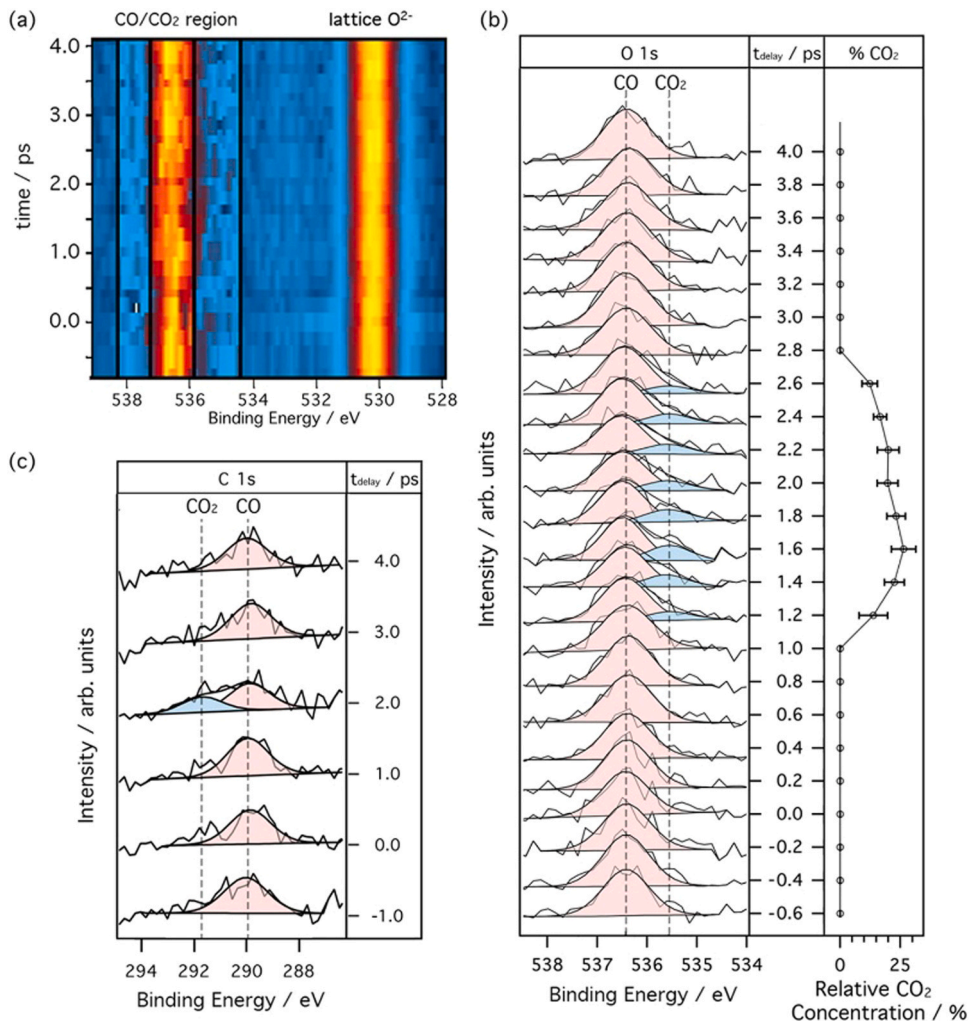
Fig. 2. TR-XPS analysis showing evidence the photo-oxidation of CO on TiO_2. A CO_2 component appears in the O 1s photoemission spectrum (b) after the optical excitation. Copyright 2020 American Chemical Society. Reprinted with permission from Ref. [88].

10^5 counts are required. The population of excited atoms/molecules is also expected to decay with the increasing delay between pump and probe pulses, thus calling for longer integration times (in the order of several hours) to effectively track the excited state dynamics. Considering the numerous possible combinations of specimens and experimental methods, it is not possible to derive a general formula for the required integration time for pump-probe measurement but the above equation can be used to roughly estimate the minimum number of counts that are necessary to detect the pump-induced signal, provided that the value of ρ_{ex} is calculated.

In this simplified formulation, we only considered local and instantaneous excitations as the origin of the time-resolved signal. However, it may happen that the effective ρ_{ex} may evolve to slightly higher values, for instance when the partial or total polarization of the system occurs [86]. In such cases the realignment of the energy levels of the sample result in spectral shifts or broadenings that become visible with relatively short integration times, as higher fractions of molecules/atoms contribute to the pump-induced signal.

3.2. Pump: the excitation density

To evaluate the excitation density of a thin film or a gas we first need to determine the number of absorbed photons, A, by means of the Beer-Lamber law:

$$A = I - T = I(1 - e^{-\alpha d}) \qquad (2)$$

where I and T are the incident and transmitted photons, assuming no reflection from the medium, α is the absorption coefficient and d is the optical path length inside the material. If A cannot be determined experimentally by measuring the optical absorption of the sample, it can be evaluated using the values from the literature for α and calculating I and d, which are based on the experimental configuration. The absorbed optical intensity can also be written in terms of the number of absorbed photons in the volume of interaction, V. From this definition we can compute the fraction of excited atoms, ρ_{ex}, by comparing such value to the molecular/atomic density of the sample, ρ_s, which is equal to the molar density of the material times the Avogadro constant:

$$\rho_{ex} = \frac{A}{V \bullet \rho_s} = I \frac{(1 - e^{-\alpha d})}{V \bullet \rho_s} \qquad (3)$$

The excitation density therefore is the ratio between the number of absorbed photons and the number of atoms or molecules in the volume of interaction, if we neglect multi-photon absorption. It should be mentioned that such estimate is valid if the lifetime of the excited state is longer than the pump pulse width and shorter than the time interval between consecutive pulses, otherwise population decay and/or build-up have to be taken into account. In the previous section we have shown that ρ_{ex} should be maximized in order to acquire high-quality pump-probe spectra with shorter integration times. With a selected
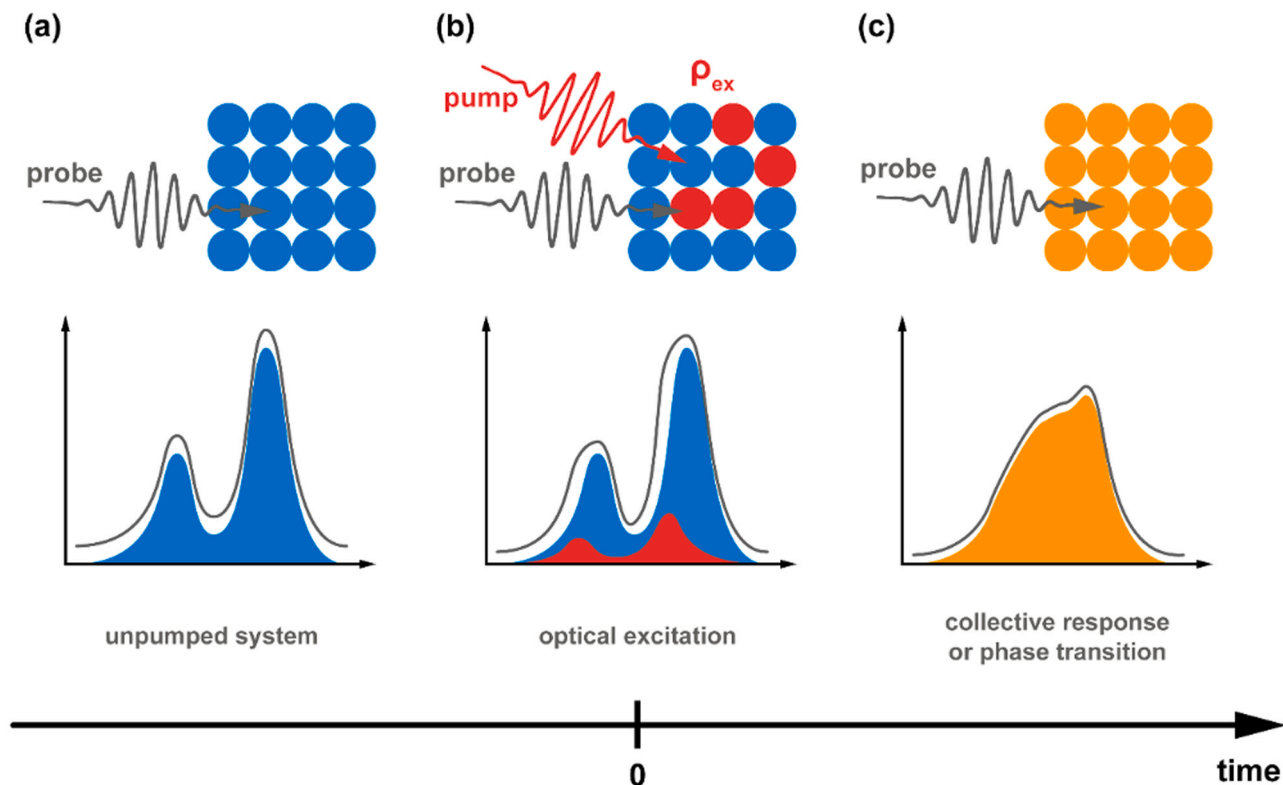
Fig. 3. Temporal evolution of a photoexcited system. (a) At negative delay times the system is unperturbed and the spectrum reflects the static picture of the sample. (b) The pump arrives on the sample at time zero; the absorbed photons excite a fraction of atoms/molecule, ρ_{ex}, which may have a different spectroscopical fingerprint than the unpumped centers, although their signal intensity is weak and scales with ρ_{ex}. (c) On a certain timescale after the optical excitation, the system may evolve into a state in which a collective response to the excitation or a phase transition has occurred on the sample, thus modifying the line shape of the entirety of the probed centers, but depicting a state that is different from the unpumped system.

sample (ρ_s, α and d are fixed), the excitation density may be in principle arbitrarily increased by increasing the pump fluence, either by acting on the laser power or on the beam focusing. However, as in the case of the probe optimization that was previously discussed, using a pump fluence over certain thresholds may cause unwanted effects to arise, such as sample heating, radiation damage, space charge emission, exciton annihilation, multi-photon absorption, thus limiting the maximum fluence that can be used for meaningful time-resolved measurements.

Gas phase samples and photon-in/photon-out detection represent the most favorable condition to avoid such issues while maximizing the excitation density. In particular, the detection of photons allows to neglect pump-induced space charge effects and the gas flow ensures that the sample is constantly regenerated, thus preventing the build-up of radiation damage features in the acquired spectra. In a recent example, Bhattacherjee et al. measured the transient X-ray absorption of acetylacetone molecules in the gas phase using an HHG source, managing to obtain an excitation percentage of ~25% [9]. Similar values of excitation density (10–20%) can be achieved when measuring the transient X-ray absorption from thin films in transmission geometry [87], with heat-induced degradation and sample ablation that determine the pump fluence threshold.

Photoemission measurements, and photon-in/electron-out spectroscopies in general, impose lower limits in the pump fluence and require more detailed analyses to successfully assign the observed effects to a specific physical process. As commented previously, the photoemitted electrons may be perturbed by transient electric fields that may arise near the sample, due to space charge photoemission or to charge transfer at interfaces, thus introducing spectral broadening and shifts in the measured spectra that may cover up the pump-induced signal. Time-resolved X-ray photoemission at the O 1 s core level has been recently used detect the photo-oxidation of CO on a TiO$_2$ substrate in the

picosecond scale [88], fully exploiting the chemical sensitivity of XPS.

As shown in Fig. 2, the authors observed the increase of signal in the CO$_2$ region, confirming that a significant amount (~20%) of CO molecules have been photo-oxidized. The chemical sensitivity of XPS allows to undeniably detect the conversion of a fraction of the carbon monoxide adsorbates to carbon anhydride, as the photoemission lines of these states lie roughly 1 eV apart. However, the vast majority of time-resolved XPS studies published in the last decade did not provide clear and unequivocal features related to the (small) local fraction of excited molecules/atoms; instead, the experimental results more frequently revealed spectral shifts or line shape modifications of the whole photoemission peaks, which were ascribed to phase transitions or to the collective response of the materials to optical excitations. In fact, the whole lineshape modification due to such effects is a more prominent feature than the few percent variation in a specific region of the photoemission spectrum, which may be related to changes in the local environment of the excited atoms; in this case, the signal may be either too weak to discriminate from the collective response of the system, or its lifetime may be shorter than the temporal resolution of the experiment. Such situation is schematically described in Fig. 3.

In addressing such issues, a remarkable progress is expected with the constant development of the present X-ray sources towards higher repetition rates and shorter pulses. Nevertheless, notable results in time-resolved XPS have been achieved in the past decade, such as the observation of phase transitions in transition metal dichalcogenides [89, 90], the characterization of charge transfer processes between inorganic [91], organic [10,12,13] and hybrid organic-inorganic [14,16] heterojunctions that are relevant for photovoltaic applications.

As an example, we have recently studied the charge transfer processes in organic heterojunctions of tetracene (Tc) and copper phthalocyanine (CuPc) grown on a Ag(111) single crystal by means of pump-
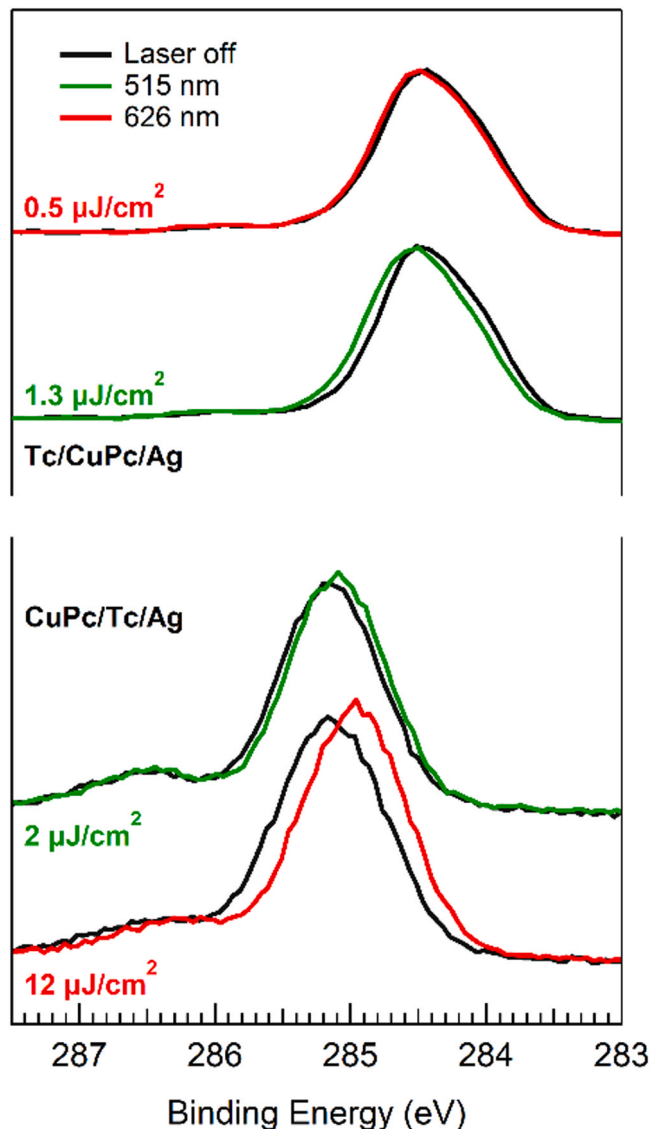
Fig. 4. Pump-probe C 1s photoemission on organic heterojunctions. Optical excitation of either of the two chromophores in the heterojunction leads to long lived spectral shifts, which are associated to the accumulation of charge carriers on the top material. Copyright 2020 American Chemical Society. Adapted with permission from Ref. [13].

probe X-ray photoemission [13]. We analyzed two different hetero-structures in which we inverted the deposition sequence of the organic films and chose two separate pump wavelengths in order to selectively pump one or the other chromophore. We found that the laser excitation induces in the C 1s peak significant energy shifts that persist for several microseconds, while allowing the system to recover to its initial state once the laser is switched off. A selection of the data is reported in Fig. 4. On top of each pumped spectrum we give the corresponding absorbed pump fluence, which has been calculated in the original paper [13]. If calculate the excitation density using these values, we find that only the 0.1% to the 2% of the chromophores are excited, yet the photoemission spectra present significant (10–100 meV) shifts, which we ascribed to the accumulation of free charge carriers on the top material after the exciton separation at the heterojunction. An important remark here concerns the sample damage: we made sure that the shifts were reversible by measuring the spectra in a laser on / laser off sequence, and we observed that the damage threshold was lower in the Tc/CuPc/Ag (111) sample (upper spectra), therefore setting the maximum achievable

ρ_{ex} to 0.1%. Clearly, such value is too low to produce within a reasonable acquisition time a measurable signal that can be directly assigned to the fraction of the excited molecules. However, the separation of the excitons and the accumulation of the charge carriers drives the system into a collectively modified state, in which the measure of the photoelectron shift can provide insights about the exciton dynamics in the heterojunction.

More generally, by examining the experimental details of the majority of time-resolved measurements reported in the literature, we may notice that the pump fluence applied on the target is in the order of 1 mJ/cm^2 at best to prevent excessive radiation damage, especially on molecular samples. We can thus attempt to generalize the maximum ρ_{ex} that is achievable, at least in the case of organic films and hetero-junctions. To use equation [3] we take α to be 0.5–1×10^5 cm^{-1}, which is a reasonable assumption for common organic films [92]; the molecular density ρ_s can be easily derived from the molar density of the selected material, and is typically around 1–3×10^{21} molecules cm^{-3}; finally, the film thickness d (or the extinction length) and the laser spot area are required to estimate the volume of interaction, V, and to convert the applied laser fluence to the actual number of photons impinging on the sample. We assume the film thickness to be in the order of 1–10 nm and the spot area to be 1×10^{-3} cm^2, corresponding to a beam diameter of 350 μm; with these parameters the 1 mJ/cm^2 fluence translates to 2–5×10^{12} photons per pulse (depending on the central wavelength). With these assumptions, we derive $\rho_{ex} \sim 0.1$: the excitation density in time-resolved X-ray spectroscopies on organic films therefore presents a 10% threshold, beyond which the sample is irreversibly damaged. To minimize radiation damage and other unwanted effects, fluences lower than 1 mJ/cm^2 are typically applied and, since the excitation density scales linearly with the latter, the fractions of optically excited molecules are most likely in the order of 1–5%. As commented previously, the signal yielded by such a small population of excited molecules is hardly distinguishable beneath the background of the remaining 95–99% unpumped molecules and it would require unpractically long integration times to measure it, however, the system may promptly evolve from the initial excited state and exhibit a collective response that results in significant and detectable changes in the spectral lineshape, which may reveal ultrafast phase transitions and charge transfer processes.

4. Conclusions

We have discussed the technical limitations of pump-probe water window soft X-ray spectroscopies, which are related in particular to the limited excitation density that is achievable without incurring in sample damage and other unwanted artifacts. In organic thin films and heter-ojunctions, which represent technologically relevant topics of research for the development of novel carbon-based optoelectronic devices, the threshold is in the order of 10%, and the typical experimental conditions in time-resolved measurement yield a percentage of excited molecules of only 1–5%. Higher excitation densities, corresponding to fractions of pumped centers in the order of 25%, may be obtained in gas phase measurements, as the sample is constantly regenerated and radiation damage can be neglected. In this case photon-in/photon-out measurements are preferred, since the higher pump fluences applied to the sample are known to introduce space charge effects that strongly perturb photoemission measurements.

We have also estimated the number of counts that are required to discriminate the pump-induced signal from the unpumped background, and we showed that it varies with ρ_{ex}^{-2}: considering the typically low values of ρ_{ex}, to detect a 1–10% pump-induced signal below the static background roughly 10^3 to 10^5 counts in the bin are required and therefore high count rates are to be preferred. To date, only synchrotron facilities can offer MHz repetition rates within the water window (280–550 eV), at the expense of a limited X-ray pulse length, which is currently in the 10–100 ps range, therefore precluding the access to faster dynamics. Sub-picosecond water window X-ray pulses are

available at FELs and HHGs which, on the other hand, offer lower repetition rates and/or higher shot-to-shot instabilities, which imply longer measurements and considerable efforts in data analysis. The constant development of pulsed X-ray sources, both towards shorter synchrotron pulses and to higher repetition rates in FELs and HHGs, will soon bring significant technological advances which will surely be beneficial for the study of ultrafast physical and chemical processes.

Declaration of Competing Interest

The authors declare that they have no known competing financial interests or personal relationships that could have appeared to influence the work reported in this paper.

Acknowledgments

References

[1] H. Petek, S. Ogawa, Femtosecond time-resolved two-photon photoemission studies of electron dynamics in metals, Prog. Surface Sci. 56 (1997) 239–310.

[2] A.H. Zewail, Femtochemistry: atomic-scale dynamics of the chemical bond, J. Phys. Chem. A 104 (2000) 5660–5694.

[3] M. Bauer, C. Lei, R. Tobey, M.M. Murnane, H. Kapteyn, Time-resolved UPS: a new experimental technique for the study of surface chemical reactions on femtosecond time-scales, Surf. Sci. 532–535 (2003) 1159–1165.

[4] O. Gessner, M. Gühr, Monitoring ultrafast chemical dynamics by time-domain X-ray photo- and auger-electron spectroscopy, Acc. Chem. Res. 49 (2016) 138–145.

[5] A. Nilsson, J. LaRue, H. Öberg, H. Ogasawara, M. Dell'Angela, M. Beye, H. Öström, J. Gladh, J.K. Nørskov, W. Wurth, F. Abild-Pedersen, L.G.M. Pettersson, Catalysis in real time using X-ray lasers, Chem. Phys. Lett. 675 (2017) 145–173.

[6] M. Dell'Angela, F. Parmigiani, M. Malvestuto, Time resolved X-ray absorption spectroscopy in condensed matter: a road map to the future, J. Electron Spectros. Relat. Phenomena 200 (2015) 22–30.

[7] R. Costantini, R. Faber, A. Cossaro, L. Floreano, A. Verdini, C. Hättig, A. Morgante, S. Coriani, M. Dell'Angela, Picosecond timescale tracking of pentacene triplet excitons with chemical sensitivity, Commun. Phys. 2 (2019) 56.

[8] H.-Y. Wang, S. Schreck, M. Weston, C. Liu, H. Ogasawara, J. LaRue, F. Perakis, M. Dell'Angela, F. Capotondi, L. Giannessi, E. Pedersoli, D. Naumenko, I. Nikolov, L. Raimondi, C. Spezzani, M. Beye, F. Cavalca, B. Liu, J. Gladh, S. Koroidov, P. S. Miedema, R. Costantini, L. Pettersson, A. Nilsson, Time-resolved observation of transient precursor state of CO on Ru(0001) using carbon K-edge spectroscopy, Phys. Chem. Chem. Phys. 22 (2020) 2677–2684.

[9] A. Bhattacherjee, C. Pemmaraju, Das, K. Schnorr, A.R. Attar, S.R. Leone, Ultrafast intersystem crossing in acetylacetone via femtosecond X-ray transient absorption at the carbon K-edge, J. Am. Chem. Soc. 139 (2017) 16576–16583.

[10] F. Roth, S. Neppl, A. Shavorskiy, T. Arion, J. Mahl, H.O. Seo, H. Bluhm, Z. Hussain, O. Gessner, W. Eberhardt, Efficient charge generation from triplet excitons in metal-organic heterojunctions, Phys. Rev. B 99 (2) (2019), 020303.

[11] S. Neppl, O. Gessner, Time-resolved X-ray photoelectron spectroscopy techniques for the study of interfacial charge dynamics, J. Electron Spectros. Relat. Phenomena 200 (2015) 64–77.

[12] F. Roth, M. Borgwardt, L. Wenthaus, J. Mahl, S. Palutke, G. Brenner, G. Mercurio, S. Molodtsov, W. Wurth, O. Gessner, W. Eberhardt, Direct observation of charge separation in an organic light harvesting system by femtosecond time-resolved XPS, Nat. Commun. 12 (2021) 1196.

[13] R. Costantini, C. Grazioli, A. Cossaro, L. Floreano, A. Morgante, M. Dell'Angela, Pump–probe X-ray photoemission reveals light-induced carrier accumulation in organic heterojunctions, J. Phys. Chem. C 124 (2020) 26603–26612.

[14] K. Ozawa, S. Yamamoto, M. D'angelo, Y. Natsui, N. Terashima, K. Mase, I. Matsuda, Enhanced photoresponsivity of fullerene in the presence of phthalocyanine: a time-resolved X-ray photoelectron spectroscopy study of phthalocyanine/C 60 /TiO 2 (110), J. Phys. Chem. C 123 (2019) 4388–4395.

[15] T. Arion, S. Neppl, F. Roth, A. Shavorskiy, H. Bluhm, Z. Hussain, O. Gessner, W. Eberhardt, Site-specific probing of charge transfer dynamics in organic photovoltaics, Appl. Phys. Lett. 106 (2015), 121602.

[16] K.R. Siefermann, C.D. Pemmaraju, S. Neppl, A. Shavorskiy, A.A. Cordones, J. Vura-Weis, D.S. Slaughter, F.P. Sturm, F. Weise, H. Bluhm, M.L. Strader, H. Cho, M. F. Lin, C. Bacellar, C. Khurmi, J. Guo, G. Coslovich, J.S. Robinson, R.A. Kaindl, R. W. Schoenlein, A. Belkacem, D.M. Neumark, S.R. Leone, D. Nordlund, H. Ogasawara, O. Krupin, J.J. Turner, W.F. Schlotter, M.R. Holmes,

[17] M. Messerschmidt, M.P. Minitti, S. Gul, J.Z. Zhang, N. Huse, D. Prendergast, O. Gessner, Atomic-scale perspective of ultrafast charge transfer at a dye–semiconductor interface, J. Phys. Chem. Lett. 5 (2014) 2753–2759.

[18] R. Schoenlein, T. Elsaesser, K. Holldack, Z. Huang, H. Kapteyn, M. Murnane, M. Woerner, Recent advances in ultrafast X-ray sources, Philos. Trans. R. Soc. A 377 (2019), 20180384.

[19] D. Attwood, Soft X-rays and extreme ultraviolet radiation: Principles and Applications, Cambridge: Cambridge University Press (1999), https://doi.org/10.1017/cbo9781139164429.

[20] Z. Chang, A. Rundquist, H. Wang, M.M. Murnane, H.C. Kapteyn, Generation of coherent soft X rays at 2.7 nm using high harmonics, Phys. Rev. Lett. 79 (1997) 2967–2970.

[21] A. Rundquist, C.G. Durfee, Z. Chang, C. Herne, S. Backus, M.M. Murnane, H. C. Kapteyn, Phase-matched generation of coherent soft x-rays, Science 280 (5368) (1998) 1412–1415.

[22] J. Seres, E. Seres, A.J. Verhoef, G. Tempea, C. Streli, P. Wobrauschek, V. Yakovlev, A. Scrinzi, C. Spielmann, F. Krausz, Source of coherent kiloelectronvolt X-rays, Nature 433 (2005) 596.

[23] M.M. Murnane, H.C. Kapteyn, M.D. Rosen, R.W. Falcone, Ultrafast X-ray Pulses from Laser-Produced Plasmas, Science 251 (4993) (1991) 531–536.

[24] M. Fuchs, R. Weingartner, A. Popp, Z. Major, S. Becker, J. Osterhoff, I. Cortrie, B. Zeitler, R. Hörlein, G.D. Tsakiris, U. Schramm, T.P. Rowlands-Rees, S.M. Hooker, D. Habs, F. Krausz, S. Karsch, F. Grüner, Laser-driven soft-X-ray undulator source, Nat. Phys. 5 (2009) 826–829.

[25] P.W. Wachulak, A. Bartnik, H. Fiedorowicz, P. Rudawski, R. Jarocki, J. Kostecki, M. Szczurek, "Water window" compact, table-top laser plasma soft X-ray sources based on a gas puff target, Nucl. Instruments Methods Phys. Res. Sect. B Beam Interact. with Mater. Atoms 268 (10) (2010) 1692–1700.

[26] U. Vogt, T. Wilhein, H. Stiel, H. Legall, High resolution x-ray absorption spectroscopy using a laser plasma radiation source, Rev. Sci. Instrum. 75 (2004) 4606–4609.

[27] S.M. Teichmann, F. Silva, S.L. Cousin, M. Hemmer, J. Biegert, 0.5-keV Soft X-ray attosecond continua, Nat. Commun. 7 (2016) 11493.

[28] I. Mantouvalou, K. Witte, W. Martyanov, A. Jonas, D. Grötzsch, C. Streeck, H. Löchel, I. Rudolph, A. Erko, H. Stiel, B. Kanngießer, Single shot near edge x-ray absorption fine structure spectroscopy in the laboratory, Appl. Phys. Lett. 108 (2016), 201106.

[29] A. Depresseux, E. Oliva, J. Gautier, F. Tissandier, G. Lambert, B. Vodungbo, J. P. Goddet, A. Tafzi, J. Nejdl, M. Kozlova, G. Maynard, H.T. Kim, K.T. Phuoc, A. Rousse, P. Zeitoun, S. Sebban, Demonstration of a circularly polarized plasma-based soft-X-ray laser, Phys. Rev. Lett. 115 (2015), 083901.

[30] H. Legall, G. Blobel, H. Stiel, W. Sandner, C. Seim, P. Takman, D.H. Martz, M. Selin, U. Vogt, H.M. Hertz, D. Esser, H. Sipma, J. Luttmann, M. Höfer, H.D. Hoffmann, S. Yulin, T. Feigl, S. Rehbein, P. Guttmann, G. Schneider, U. Wiesemann, M. Wirtz, W. Diete, Compact x-ray microscope for the water window based on a high brightness laser plasma source, Opt. Express 20 (2012) 18362–18369.

[31] P. Wachulak, M. Duda, A. Bartnik, Ł. Węgrzyński, T. Fok, H. Fiedorowicz, NEXAFS at nitrogen K-edge and titanium L-edge using a laser-plasma soft x-ray source based on a double-stream gas puff target, APL Photonics 4 (2019), 030807.

[32] I. Mantouvalou, R. Jung, J. Tuemmler, H. Legall, T. Bidu, H. Stiel, W. Malzer, B. Kanngiesser, W. Sandner, Note: Study of extreme ultraviolet and soft x-ray emission of metal targets produced by laser-plasma-interaction, Rev. Sci. Instrum. 82 (2011), 066103.

[33] I. Mantouvalou, K. Witte, D. Grötzsch, M. Neitzel, S. Günther, J. Baumann, R. Jung, H. Stiel, B. Kanngiesser, W. Sandner, High average power, highly brilliant laser-produced plasma source for soft X-ray spectroscopy, Rev. Sci. Instrum. 86 (2015), 035116.

[34] S.J. Haney, K.W. Berger, G.D. Kubiak, P.D. Rockett, J. Hunter, Prototype high-speed tape target transport for a laser plasma soft-x-ray projection lithography source, Appl. Opt 32 (34) (1993) 6934–6937.

[35] M. Beck, U. Vogt, I. Will, A. Liero, H. Stiel, W. Sandner, T. Wilhein, A pulse-train laser driven XUV source for picosecond pump–probe experiments in the water window, Opt. Commun. 190 (1–6) (2001) 317–326.

[36] J. Andruszkow, B. Aune, V. Ayvazyan, N. Baboi, R. Bakker, V. Balakin, D. Barni, A. Bazhan, M. Bernard, A. Bosotti, J.C. Bourdon, W. Brefeld, R. Brinkmann, S. Buhler, J.P. Carneiro, M. Castellano, P. Castro, L. Catani, S. Chel, Y. Cho, S. Choroba, E.R. Colby, W. Decking, P. Den Hartog, M. Desmons, M. Dohlus, D. Edwards, H.T. Edwards, B. Faatz, J. Feldhaus, M. Ferrario, M.J. Fitch, K. Flöttmann, A. Fouaidy, A. Gamp, T. Garvey, C. Gerth, M. Geitz, E. Gluskin, V. Gretchko, U. Hahn, W.H. Hartung, D. Hubert, M. Hüning, R. Ischebeck, M. Jablonka, J.M. Joly, M. Juillard, T. Junquera, P. Jurkiewicz, A. Kabel, J. Kahl, H. Kaiser, T. Kamps, V.V. Katelev, J.L. Kirchgessner, M. Körfer, L. Kravchuk, G. Kreps, J. Krzywinski, T. Lokajczyk, R. Lange, B. Leblond, M. Leenen, J. Lesrel, M. Liepe, A. Liero, T. Limberg, R. Lorenz, L.H. Hua, L.F. Hai, C. Magne, M. Maslov, G. Materlik, A. Matheisen, J. Menzel, P. Michelato, W.D. Möller, A. Mosnier, U. C. Müller, O. Napoly, A. Novokhatski, M. Omeich, H.S. Padamsee, C. Pagani, F. Peters, B. Petersen, P. Pierini, J. Pflüger, P. Piot, B. Phung Ngoc, L. Plucinski, D. Proch, K. Rehlich, S. Reiche, D. Reschke, I. Reyzl, J. Rosenzweig, J. Rossbach, S. Roth, E.L. Saldin, W. Sandner, Z. Sanok, H. Schlarb, G. Schmidt, P. Schmüser, J. R. Schneider, E.A. Schneidmiller, H.J. Schreiber, S. Schreiber, P. Schütt, J. Sekutowicz, L. Serafini, D. Sertore, S. Setzer, S. Simrock, B. Sonntag, B. Sparr, F. Stephan, V.A. Sytchev, S. Tazzari, F. Tazzioli, M. Tigner, M. Timm, M. Tonutti, E. Trakhtenberg, R. Treusch, D. Trines, V. Verzilov, T. Vielitz, V. Vogel, G. Walter, R. Wanzenberg, T. Weiland, H. Weise, J. Weisend, M. Wendt, M. Werner, M.

M. White, I. Will, S. Wolff, M.V. Yurkov, K. Zapfe, P. Zhogolev, F. Zhou, First observation of self-amplified spontaneous emission in a free-electron laser at 109 nm wavelength, Phys. Rev. Lett. 85 (2000) 3825–3829.

[37] Z. Huang, K.-J. Kim, Review of x-ray free-electron laser theory, Phys. Rev. Spec. Top. Accel. Beams 10 (2007), 034801.

[38] R. Costantini, M. Stredansky, D. Cvetko, G. Kladnik, A. Verdini, P. Sigalotti, F. Cilento, F. Salvador, A. De Luisa, D. Benedetti, L. Floreano, A. Morgante, A. Cossaro, M. Dell'Angela, ANCHOR-SUNDYN: a novel endstation for time resolved spectroscopy at the ALOISA beamline, J. Electron Spectros. Relat. Phenomena 229 (2018) 7–12.

[39] M. Ogawa, S. Yamamoto, Y. Kousa, F. Nakamura, R. Yukawa, A. Fukushima, A. Harasawa, H. Kondoh, Y. Tanaka, A. Kakizaki, I. Matsuda, Development of soft x-ray time-resolved photoemission spectroscopy system with a two-dimensional angle-resolved time-of-flight analyzer at SPring-8 BL07LSU, Rev. Sci. Instrum. 83 (2012), 023109.

[40] N. Bergeard, M.G. Silly, D. Krizmancic, C. Chauvet, M. Guzzo, J.P. Ricaud, M. Izquierdo, L. Stebel, P. Pittana, R. Sergo, G. Cautero, G. Dufour, F. Rochet, F. Sirotti, Time-resolved photoelectron spectroscopy using synchrotron radiation time structure, J. Synchrotron Radiat. 18 (2011) 245–250.

[41] M. Krebs, S. Hädrich, S. Demmler, J. Rothhardt, A. Zaïr, L. Chipperfield, J. Limpert, A. Tünnermann, Towards isolated attosecond pulses at megahertz repetition rates, Nat. Photonics 7 (2013) 555–559.

[42] A. Harth, C. Guo, Y.C. Cheng, A. Losquin, M. Miranda, S. Mikaelsson, C.M. Heyl, O. Prochnow, J. Ahrens, U. Morgner, A. L'Huillier, C.L. Arnold, Compact 200 kHz HHG source driven by a few-cycle OPCPA, J. Opt. 20 (2018), 014007.

[43] T. Popmintchev, M.-C. Chen, P. Arpin, M.M. Murnane, H.C. Kapteyn, The attosecond nonlinear optics of bright coherent X-ray generation, Nat. Photonics 4 (2010) 822–832.

[44] M.-C. Chen, P. Arpin, T. Popmintchev, M. Gerrity, B. Zhang, M. Seaberg, D. Popmintchev, M.M. Murnane, H.C. Kapteyn, Bright, Coherent, Ultrafast Soft X-Ray Harmonics Spanning the Water Window from a Tabletop Light Source, Phys. Rev. Lett. 105 (2010), 173901.

[45] T. Popmintchev, M.C. Chen, D. Popmintchev, P. Arpin, S. Brown, S. Alisauskas, G. Andriukaitis, T. Balciunas, O.D. Mücke, A. Pugzlys, A. Baltuska, B. Shim, S. E. Schrauth, A. Gaeta, C. Hernández-García, L. Plaja, A. Becker, A. Jaron-Becker, M.M. Murnane, H.C. Kapteyn, Bright coherent ultrahigh harmonics in the keV X-ray regime from mid-infrared femtosecond lasers, Science 336 (6086) (2012) 1287–1291.

[46] L. Barreau, A.D. Ross, S. Garg, P.M. Kraus, D.M. Neumark, S.R. Leone, Efficient table-top dual-wavelength beamline for ultrafast transient absorption spectroscopy in the soft X-ray region, Sci. Rep. 10 (2020) 5773.

[47] C. Kleine, M. Ekimova, G. Goldsztejn, S. Raabe, C. Strüber, J. Ludwig, S. Yarlagadda, S. Eisebitt, M. Vrakking, T. Elsaesser, E. Nibbering, A. Rouzée, Soft X-ray absorption spectroscopy of aqueous solutions using a table-top femtosecond soft X-ray source, J. Phys. Chem. Lett. 10 (2019) 52–58.

[48] E.J. Takahashi, T. Kanai, K.L. Ishikawa, Y. Nabekawa, K. Midorikawa, Coherent water window X ray by phase-matched high-order harmonic generation in neutral media, Phys. Rev. Lett. 101 (2008), 253901.

[49] J. Li, X. Ren, Y. Yin, K. Zhao, A. Chew, Y. Cheng, E. Cunningham, Y. Wang, S. Hu, Y. Wu, M. Chini, Z. Chang, 53-attosecond X-ray pulses reach the carbon K-edge, Nat. Commun. 8 (2017), 186.

[50] T. Feng, A. Heilmann, M. Bock, L. Ehrentraut, T. Witting, H. Yu, H. Stiel, S. Eisebitt, M. Schnürer, 27 W 21 μm OPCPA system for coherent soft X-ray generation operating at 10 kHz, Opt. Express 28 (6) (2020) 8724–8733.

[51] A.S. Johnson, D.R. Austin, D.A. Wood, C. Brahms, A. Gregory, K.B. Holzner, S. Jarosch, E.W. Larsen, S. Parker, C.S. Strüber, P. Ye, J. Tisch, J.P. Marangos, High-flux soft x-ray harmonic generation from ionization-shaped few-cycle laser pulses, Sci. Adv. 4 (5) (2018) 3761.

[52] S.L. Cousin, F. Silva, S. Teichmann, M. Hemmer, B. Buades, J. Biegert, High-flux table-top soft x-ray source driven by sub-2-cycle, CEP stable, 185 μm 1 kHz pulses for carbon K-edge spectroscopy, Opt. Lett. 39 (2014) 5383–5386.

[53] C. Schmidt, Y. Pertot, T. Balciunas, K. Zinchenko, M. Matthews, H.J. Wörner, J. P. Wolf, High-order harmonic source spanning up to the oxygen K-edge based on filamentation pulse compression, Opt. Express 26 (9) (2018) 11834–11842.

[54] E.A. Gibson, A. Paul, N. Wagner, R. Tobey, D. Gaudiosi, S. Backus, I.P. Christov, A. Aquila, E.M. Gullikson, D.T. Attwood, M.M. Murnane, H.C. Kapteyn, Coherent soft x-ray generation in the water window with quasi-phase matching, Science 302 (5642) (2003) 95–98.

[55] Y. Pertot, C. Schmidt, M. Matthews, A. Chauvet, M. Huppert, V. Svoboda, A. von Conta, A. Tehlar, D. Baykusheva, J.P. Wolf, H.J. Wörner, Time-resolved x-ray absorption spectroscopy with a water window high-harmonic source, Science 355 (6322) (2017) 264–267.

[56] Y. Fu, K. Nishimura, R. Shao, A. Suda, K. Midorikawa, P. Lan, E.J. Takahashi, High efficiency ultrafast water-window harmonic generation for single-shot soft X-ray spectroscopy, Commun. Phys. 3 (2020) 92.

[57] V. Cardin, B.E. Schmidt, N. Thiré, S. Beaulieu, V. Wanie, M. Negro, C. Vozzi, V. Tosa, F. Légaré, Self-channelled high harmonic generation of water window soft x-rays, J. Phys. B Atom. Mol. Opt. Phys. 51 (2018), 174004.

[58] E. Goulielmakis, Z.H. Loh, A. Wirth, R. Santra, N. Rohringer, V.S. Yakovlev, S. Zherebtsov, T. Pfeifer, A.M. Azzeer, M.F. Kling, S.R. Leone, F. Krausz, Real-time observation of valence electron motion, Nature 466 (2010) 739–743.

[59] M. Schultze, K. Ramasesha, C.D. Pemmaraju, S.A. Sato, D. Whitmore, A. Gandman, J.S. Prell, L.J. Borja, D. Prendergast, K. Yabana, D.M. Neumark, S.R. Leone, Attosecond band-gap dynamics in silicon, Science 346 (6215) (2014) 1348–1352.

[60] M. Gebhardt, T. Heuermann, R. Klas, C. Liu, A. Kirsche, M. Lenski, Z. Wang, C. Gaida, J.E. Antonio-Lopez, A. Schülzgen, R. Amezcua-Correa, J. Rothhardt,

[61] J. Limpert, Bright, high-repetition-rate water window soft X-ray source enabled by nonlinear pulse self-compression in an antiresonant hollow-core fibre, Light Sci. Appl. 10 (2021) 36.

[61] P. Emma, R. Akre, J. Arthur, R. Bionta, C. Bostedt, J. Bozek, A. Brachmann, P. Bucksbaum, R. Coffee, F.J. Decker, Y. Ding, D. Dowell, S. Edstrom, A. Fisher, J. Frisch, S. Gilevich, J. Hastings, G. Hays, P. Hering, Z. Huang, R. Iverson, H. Loos, M. Messerschmidt, A. Miahnahri, S. Moeller, H.D. Nuhn, G. Pile, D. Ratner, J. Rzepiela, D. Schultz, T. Smith, P. Stefan, H. Tompkins, J. Turner, J. Welch, W. White, J. Wu, G. Yocky, J. Galayda, First lasing and operation of an ångstrom-wavelength free-electron laser, Nat. Photonics 4 (2010) 641–647.

[62] M. Yabashi, H. Tanaka, T. Ishikawa, Overview of the SACLA facility, J. Synchrotron Radiat 22 (2015) 477–484.

[63] B.D. Patterson, R. Abela, H.H. Braun, U. Flechsig, R. Ganter, Y. Kim, E. Kirk, A. Oppelt, M. Pedrozzi, S. Reiche, L. Rivkin, T. Schmidt, B. Schmitt, V.N. Strocov, S. Tsujino, A.F. Wrulich, Coherent science at the SwissFEL x-ray laser, New J. Phys. 12 (2010), 035012.

[64] S. Hellmann, C. Sohrt, M. Beye, T. Rohwer, F. Sorgenfrei, M. Marczynski-Bühlow, M. Kalläne, H. Redlin, F. Hennies, M. Bauer, A. Föhlisch, L. Kipp, W. Wurth, K. Rossnagel, Time-resolved x-ray photoelectron spectroscopy at FLASH, New J. Phys. 14 (2012), 013062.

[65] E. Allaria, R. Appio, L. Badano, W.A. Barletta, S. Bassanese, S.G. Biedron, A. Borga, E. Busetto, D. Castronovo, P. Cinquegrana, S. Cleva, D. Cocco, M. Cornacchia, P. Craievich, I. Cudin, G. D'Auria, M. Dal Forno, M.B. Danailov, R. De Monte, G. De Ninno, P. Delgiusto, A. Demidovich, S. Di Mitri, B. Diviacco, A. Fabris, R. Fabris, W. Fawley, M. Ferianis, E. Ferrari, S. Ferry, L. Froehlich, P. Furlan, G. Gaio, F. Gelmetti, L. Giannessi, M. Giannini, R. Gobessi, R. Ivanov, E. Karantzoulis, M. Lonza, A. Lutman, B. Mahieu, M. Milloch, S.V. Milton, M. Musardo, I. Nikolov, S. Noe, F. Parmigiani, G. Penco, M. Petronio, L. Pivetta, M. Predonzani, F. Rossi, L. Rumiz, A. Salom, C. Scafuri, C. Serpico, P. Sigalotti, S. Spampinati, C. Spezzani, M. Svandrlik, C. Svetina, S. Tazzari, M. Trovo, R. Umer, A. Vascotto, M. Veronese, R. Visintini, M. Zaccaria, D. Zangrando, M. Zangrando, Highly coherent and stable pulses from the FERMI seeded free-electron laser in the extreme ultraviolet, Nat. Photonics 6 (2012) 699–704.

[66] H.N. Chapman, P. Fromme, A. Barty, T.A. White, R.A. Kirian, A. Aquila, M. S. Hunter, J. Schulz, D.P. DePonte, U. Weierstall, R.B. Doak, F.R. Maia, A.V. Martin, I. Schlichting, L. Lomb, N. Coppola, R.L. Shoeman, S.W. Epp, R. Hartmann, D. Rolles, A. Rudenko, L. Foucar, N. Kimmel, G. Weidenspointner, P. Holl, M. Liang, M. Barthelmess, C. Caleman, S. Boutet, M.J. Bogan, J. Krzywinski, C. Bostedt, S. Bajt, L. Gumprecht, B. Rudek, B. Erk, C. Schmidt, A. Hömke, C. Reich, D. Pietschner, L. Strüder, G. Hauser, H. Gorke, J. Ullrich, S. Herrmann, G. Schaller, F. Schopper, H. Soltau, K.U. Kühnel, M. Messerschmidt, J.D. Bozek, S.P. Hau-Riege, M. Frank, C.Y. Hampton, R.G. Sierra, D. Starodub, G.J. Williams, J. Hajdu, N. Timneanu, M.M. Seibert, J. Andreasson, A. Rocker, O. Jönsson, M. Svenda, S. Stern, K. Nass, R. Andritschke, C.D. Schröter, F. Krasniqi, M. Bott, K.E. Schmidt, X. Wang, I. Grotjohann, J.M. Holton, T.R. Barends, R. Neutze, S. Marchesini, R. Fromme, S. Schorb, D. Rupp, M. Adolph, T. Gorkhover, I. Andersson, H. Hirsemann, G. Potdevin, H. Graafsma, B. Nilsson, J.C. Spence, Femtosecond X-ray protein nanocrystallography, Nature 470 (2011) 73–77.

[67] S. Boutet, L. Lomb, G.J. Williams, T.R. Barends, A. Aquila, R.B. Doak, U. Weierstall, D.P. DePonte, J. Steinbrener, R.L. Shoeman, M. Messerschmidt, A. Barty, T. A. White, S. Kassemeyer, R.A. Kirian, M.M. Seibert, P.A. Montanez, C. Kenney, R. Herbst, P. Hart, J. Pines, G. Haller, S.M. Gruner, H.T. Philipp, M.W. Tate, M. Hromalik, L.J. Koerner, N. van Bakel, J. Morse, W. Ghonsalves, D. Arnlund, M. J. Bogan, C. Caleman, R. Fromme, C.Y. Hampton, M.S. Hunter, L.C. Johansson, G. Katona, C. Kupitz, M. Liang, A.V. Martin, K. Nass, L. Redecke, F. Stellato, N. Timneanu, D. Wang, N.A. Zatsepin, D. Schafer, J. Defever, R. Neutze, P. Fromme, J.C. Spence, H.N. Chapman, I. Schlichting, High-Resolution Protein Structure Determination by Serial Femtosecond Crystallography, Science 337 (6092) (2012) 362–364.

[68] S. Hellmann, K. Rossnagel, M. Marczynski-Bühlow, L. Kipp, Vacuum space-charge effects in solid-state photoemission, Phys. Rev. B 79 (2009), 035402.

[69] X.J. Zhou, B. Wannberg, W.L. Yang, V. Brouet, Z. Sun, J.F. Douglas, D. Dessau, Z. Hussain, Z.X. Shen, Space charge effect and mirror charge effect in photoemission spectroscopy, J. Electron Spectros. Relat. Phenomena 142 (2005) 27–38.

[70] M. Dell'Angela, T. Anniyev, M. Beye, R. Coffee, A. Föhlisch, J. Gladh, S. Kaya, T. Katayama, O. Krupin, A. Nilsson, D. Nordlund, W.F. Schlotter, J.A. Sellberg, F. Sorgenfrei, J.J. Turner, H. Öström, H. Ogasawara, M. Wolf, W. Wurth, Vacuum space charge effects in sub-picosecond soft X-ray photoemission on a molecular adsorbate layer, Struct. Dyn. 2 (2015), 025101.

[71] M. Altarelli, The European X-ray Free-Electron Laser: toward an ultra-bright, high repetition-rate x-ray source, High Power Laser Sci. Eng 3 (e18) (2015) 1–7.

[72] P. Emma, J. Frisch, Z. Huang, A. Marinelli, T. Maxwell, H. Loos, Y. Nosochkov, T. Raubenheimer, J. Welch, L. Wang, M. Woodley, A. Saini, N. Solyak, J. Qiang, M. Venturini, Linear accelerator design for the LCLS-II FEL facility, Proc. 36th Int. Free Electron Laser Conf. FEL 2014 (2014) 743–747.

[73] Feikes J., Holldack K., Kuske P. Sub-picosecond Electron Bunches in the BESSY Storage Ring. in Proceedings of EPAC 2004 1954–1956 (2004).

[74] C. Steier, P. Heimann, S. Marks, D. Robin, R. Schoenlein, W. Wan, W. Wittmer. Successful completion of the femtosecond slicing upgrade at the ALS, IEEE, 2007, pp. 1194–1196.

[75] A. Zholents, P. Heimann, M. Zolotorev, J. Byrd, Generation of subpicosecond X-ray pulses using RF orbit deflection, Nucl. Instruments Methods Phys. Res. Sect. A Accel. Spectrometers Detect. Assoc. Equip. 425 (1999) 385–389.

[76] V. Sajaev, M. Borland, Y.C. Chae, G. Decker, R. Dejus, L. Emery, K. Harkay, A. Nassiri, S. Shastri, G. Waldschmidt, B. Yang, P. Anfinrud, V. Dolgashev, Short X-

ray pulse generation using deflecting cavities at the Advanced Photon Source, Nucl. Instruments Methods Phys. Res. Sect. A Accel. Spectrometers Detect. Assoc. Equip. 582 (2007) 57–59.

[77] R.W. Schoenlein, S. Chattopadhyay, H.H. Chong, T.E. Glover, P.A. Heimann, C. V. Shank, A.A. Zholents, M.S. Zolotorev, Generation of femtosecond pulses of synchrotron radiation, Science 287 (5461) (2000) 2237–2240.

[78] S. Khan, K. Holldack, T. Kachel, R. Mitzner, T. Quast, Femtosecond undulator radiation from sliced electron bunches, Phys. Rev. Lett. 97 (2006), 074801.

[79] P. Beaud, S.L. Johnson, A. Streun, R. Abela, D. Abramsohn, D. Grolimund, F. Krasniqi, T. Schmidt, V. Schlott, G. Ingold, Spatiotemporal stability of a femtosecond hard–X-ray undulator source studied by control of coherent optical phonons, Phys. Rev. Lett. 99 (2007), 174801.

[80] M. Labat, J.B. Brubach, A. Ciavardini, M.E. Couprie, E. Elkaim, P. Fertey, T. Ferte, P. Hollander, N. Hubert, E. Jal, C. Laulhé, J. Luning, O. Marcouillé, T. Moreno, P. Morin, F. Polack, P. Prigent, S. Ravy, J.P. Ricaud, P. Roy, M. Silly, F. Sirotti, A. Taleb, M.A. Tordeux, A. Nadji, Commissioning of a multi-beamline femtoslicing facility at SOLEIL, J. Synchrotron Radiat. 25 (2018) 385–398.

[81] A. Jankowiak, W. Anders, T. Atkinson, H. Ehmler, A. Föhlisch, P. Goslawski, K. Holldack, J. Knobloch, P. Kuske, D. Malyutin, A. Matveenko, R. Müller, A. Neumann, M. Ott, M. Ries, M. Ruprecht, A. Schälicke, A. Velez, G. Wüstefeld, A. Burrill, The BESSY VSR project for short X-ray pulse production. IPAC 2016 -, Proc. 7th Int. Part. Accel. Conf. 2833–2836 (2016).

[82] J. Maklar, S. Dong, S. Beaulieu, T. Pincelli, M. Dendzik, Y.W. Windsor, R.P. Xian, M. Wolf, R. Ernstorfer, L. Rettig, A quantitative comparison of time-of-flight momentum microscopes and hemispherical analyzers for time- and angle-resolved photoemission spectroscopy experiments, Rev. Sci. Instrum. 91 (2020), 123112.

[83] R.P. Xian, Y. Acremann, S.Y. Agustsson, M. Dendzik, K. Bühlmann, D. Curcio, D. Kutnyakhov, F. Pressacco, M. Heber, S. Dong, T. Pincelli, J. Demsar, W. Wurth, P. Hofmann, M. Wolf, M. Scheidgen, L. Rettig, R. Ernstorfer, An open-source, end-to-end workflow for multidimensional photoemission spectroscopy, Sci. Data 7 (2020), 442.

[84] C. Svetina, R. Mankowsky, G. Knopp, F. Koch, G. Seniutinas, B. Rösner, A. Kubec, M. Lebugle, I. Mochi, M. Beck, C. Cirelli, J. Krempasky, C. Pradervand, J. Rouxel, G.F. Mancini, S. Zerdane, B. Pedrini, V. Esposito, G. Ingold, U. Wagner, U. Flechsig,

[85] R. Follath, M. Chergui, C. Milne, H.T. Lemke, C. David, P. Beaud, Towards X-ray transient grating spectroscopy, Opt. Lett. 44 (2019) 574–577.

[85] D. Kühn, E. Giangrisostomi, R.M. Jay, F. Sorgenfrei, A. Föhlisch, The influence of x-ray pulse length on space-charge effects in optical pump/x-ray probe photoemission, New J. Phys. 21 (2019), 073042.

[86] B. Stadtmüller, S. Emmerich, D. Jungkenn, N. Haag, M. Rollinger, S. Eich, M. Maniraj, M. Aeschlimann, M. Cinchetti, S. Mathias, Strong modification of the transport level alignment in organic materials after optical excitation, Nat. Commun. 10 (2019) 1470.

[87] E.S. Ryland, K. Zhang, J. Vura-Weis, Sub-100 fs intersystem crossing to a metal-centered triplet in Ni(II)OEP observed with M-edge XANES, J. Phys. Chem. A 123 (2019) 5214–5222.

[88] M. Wagstaffe, L. Wenthaus, A. Dominguez-Castro, S. Chung, G.D. Lana Semione, S. Palutke, G. Mercurio, S. Dziarzhytski, H. Redlin, N. Klemke, Y. Yang, T. Frauenheim, A. Dominguez, F. Kärtner, A. Rubio, W. Wurth, A. Stierle, H. Noei, Ultrafast real-time dynamics of CO oxidation over an oxide photocatalyst, ACS Catal. 10 (2020) 13650–13658.

[89] S. Hellmann, M. Beye, C. Sohrt, T. Rohwer, F. Sorgenfrei, H. Redlin, M. Kalläne, M. Marczynski-Bühlow, F. Hennies, M. Bauer, A. Föhlisch, L. Kipp, W. Wurth, K. Rossnagel, Ultrafast melting of a charge-density wave in the mott insulator 1T-TaS2, Phys. Rev. Lett. 105 (2010), 187401.

[90] M. Dendzik, R.P. Xian, E. Perfetto, D. Sangalli, D. Kutnyakhov, S. Dong, S. Beaulieu, T. Pincelli, F. Pressacco, D. Curcio, S.Y. Agustsson, M. Heber, J. Hauer, W. Wurth, G. Brenner, Y. Acremann, P. Hofmann, M. Wolf, A. Marini, G. Stefanucci, L. Rettig, R. Ernstorfer, Observation of an excitonic mott transition through ultrafast core-cum-conduction photoemission spectroscopy, Phys. Rev. Lett. 125 (2020), 096401.

[91] C. Gréboval, P. Rastogi, J. Qu, A. Chu, J. Ramade, A. Khalili, C. Dabard, T.H. Dang, H. Cruguel, A. Ouerghi, N. Witkowski, M.G. Silly, E. Lhuillier, Time-resolved photoemission to unveil electronic coupling between absorbing and transport layers in a quantum dot-based solar cell, J. Phys. Chem. C 124 (2020) 23400–23409.

[92] J. Huang, J. Yu, Z. Guan, Y. Jiang, Improvement in open circuit voltage of organic solar cells by inserting a thin phosphorescent iridium complex layer, Appl. Phys. Lett. 97 (2010), 143301.